Formulation and characterization of the biological activities of green synthesized zinc oxide nanoparticles from *Annona muricata* leaf extract

Titilayomi Olufunso Olutoyin Adewusi*[1,3] and Ovgu Isbilen[1,2,3]

[1]Faculty of Pharmacy, Cyprus International University, Nicosia, Northern Cyprus, via Mersin, Turkey
[2]Faculty of Art and Sciences, Cyprus International University, Nicosia, Northern Cyprus, via Mersin, Turkey
[3]Biotechnology Research Center, Cyprus International University, Nicosia, Northern Cyprus, via Mersin, Turkey

Abstract: *Annona muricata* belongs to the family Annonaceae and the leaf extract has traditionally been used as an antipyretic, anti-diabetic, antihypertensive, and antimalarial. The study aims to formulate zinc oxide nanoparticles (ZnO NPs) using *Annona muricata* leaf extract (AME) and evaluate its biological activities. The biosynthesized ZnO NPs were characterized using UV-vis spectroscopy, FTIR, XRD and SEM. GC-MS analysis of AME indicated sesquiterpenes, acetogenins, alkaloids, flavonoids, fatty acids and other compounds. The presence of ZnONPs was confirmed by the UV-vis absorption spectrum with a peak at 370 nm. XRD and FTIR showed the stabilized ZnO NPs using AME bioactive compounds with an average particle size of 79.14 nm. SEM and EDX revealed spherical and hexagonal morphology. Minimum inhibitory concentration experiments revealed that MIC values for *P. aeruginosa* and *B. subtilis* were 1.25mg/mL and 0.32mg/mL, respectively. Antioxidant activities of the AME, AME-ZnO NPs and ascorbic acid (standard) using DPPH assay revealed IC_{50} values of 2.17mg/mL, 1.66mg/mL and 0.23mg/mL, respectively. The formulated ZnO NPs also aided in the photocatalysis of methylene blue at a degradation rate of 66.8% after 180 min. These results collectively highlight the promising therapeutic potential of *A. muricata* biogenic zinc oxide nanoparticles for developing future therapies due to antibacterial, photocatalytic and antioxidant activities.

Keywords: *Annona muricata*, antibacterial, antioxidant, photocatalysis, zinc oxide nanoparticles

INTRODUCTION

Drugs derived from medicinal plants have been pivotal in healthcare throughout human history. A significant portion of the world population relies on plant-based medicinal practices that utilize plant-based therapeutics (Dias *et al*., 2012). Additionally, the World Health Organization (WHO) has reported that around 80% of the global population depends on medicinal-originated drugs, thus highlighting their importance and efficacy in various communities (Sen and Samanta, 2014).

A. muricata, belonging to the Annonaceae family, is also known by many names, such as "Soursop," "Graviola," and "Guanabana," and is commonly found in Asia, Africa, and South America. Its leaves have long been used in traditional medicine for their antipyretic, sedative, anti-diabetic, antihypertensive, antidepressant and antimalarial properties. (Karthik *et al*., 2023). Various parts of *A. muricata*, such as the seeds, roots, bark and fruits, have also demonstrated significant pharmacological activity, making it an integral part of ethnomedicine for treating bacterial and fungal infections, inflammation, diabetes and gastroenteritis (Kumaran *et al*., 2021). The bioactive molecules found in AME, including alkaloids, flavonoids, acetogenins, and other secondary metabolites, have been reported by previous research to exhibit significant biological activities relating to antimicrobial, anti-inflammatory, antitumor, antioxidant, cytotoxicity, anti-protozoal, antiparasitic, larvicidal, anxiolytic, antiulcer, hepatoprotective and hypoglycemic properties (Mutakin *et al*., 2022, Afroz *et al*., 2020).

Previous studies revealed that zinc is used therapeutically as a wound healing agent in patients with severe burns, as treatment of diarrhea in children, and is also very important in their growth and central nervous system, DNA synthesis, cell division, bone metabolism, and the immune system (Muhtadi *et al*., 2023). Studies on zinc ions report the presence of significant antimicrobial and antioxidant activities with antiaging properties. Glutamatergic neurons in the brain use specific synaptic vesicles to store zinc in the body; hence, it plays an important function in synaptic plasticity, memory, cognition and learning. Zinc homeostasis is vital in the brain and spinal cord (Stiles *et al*., 2024). However, zinc deficiency usually occurs due to reduced zinc in the body or inadequate zinc ingestion or absorption, which may be associated with malabsorption, chronic liver and kidney disease, sickle cell anemia, diabetes, etc. Zinc deficiency has been reported to cause an increase in susceptibility to infection as well as diarrhea in children, leading to the mortality of about 800,000 children globally every year; hence, the World Health Organization (WHO) advocates supplementation of zinc for the treatment of severe diarrhea and malnutrition in children (Monfared *et al*., 2023).

Corresponding author: e-mail: titilayomiadewusi@gmail.com

The utilization of biocompatible and environmentally stable nanoparticles in healthcare and environmental applications is gaining prominence, with metal oxides such as ZnO, CuO, MgO and TiO2 being preferred for their cost-effectiveness and therapeutic potential (Reid *et al.*, 2018). Among them, zinc oxide nanoparticles (ZnONPs) stand out for their strong antimicrobial and antioxidant effects and their utility in environmental photocatalysis (Muhtadi *et al.*, 2023). ZnO is considered an outstanding biocompatible material. It can be absorbed into the bloodstream as either particles or ions due to its high solubility in the acidic conditions of the stomach as well as in the fluid lining of the respiratory tract. Once absorbed, ZnO is quickly metabolized by cytochrome P450 enzymes in the liver and then redistributed to various tissues, enhancing its suitability for applications such as antimicrobial and cancer treatments, tissue engineering and environmental photocatalysis to help reduce pollutants and minimize environmental footprint (Fujihara and Nishimoto, 2024).

However, traditional chemical methods of synthesizing ZnONPs present significant environmental and biocompatibility risks. Previous studies on ZnO nanoparticles have demonstrated their immense potential, particularly in antimicrobial and antioxidant applications, but their synthesis through chemical methods poses significant environmental challenges. Chemical synthesis can release toxic by-products that can bioaccumulate in aquatic ecosystems, causing oxidative stress in organisms and potentially leading to ecological imbalances (Bhattacharjee *et al.*, 2024). Although ZnO NPs hold significant therapeutic potential, various concerns regarding their safety, especially related to cytotoxicity, have been raised. ZnO NPs have been reported to cause inflammation and oxidative stress in mammalian cells, particularly when administered in higher doses. Inhalation exposure has also been linked to respiratory toxicity and the increasing risk of chronic conditions such as lung fibrosis (Ahmed *et al.*, 2023). These limitations highlight the need for a safer and alternative synthesis methods. To address these issues, biogenic synthesis using plant extracts has gained attention as a safer, eco-friendly and biocompatible alternative that eliminates harmful chemicals and enhances the safety of the nanoparticles. Despite these advantages, challenges, such as controlling the nanoparticle shape, size and yield, continue to limit scalability. However, green synthesis methods hold great potential for producing nanoparticles with high therapeutic efficacy and minimal environmental impact (Reid *et al.*, 2023).

The therapeutic potency of *A. muricata* leaves and fruit used in the formulation of nanoparticles has been demonstrated with gold, silver and zinc nanoparticles as reducing and capping agents. In a study by Karthik *et al*, zinc oxide nanoparticles synthesized from *A. muricata* leaf extract, obtained an optimum inhibitory level of 240µg/mL against the bacterial isolates used (Karthik *et al.,* 2023). Similarly, Selvanathan *et al*, synthesized ZnO nanoparticles from soursop leaf extracts investigated its cytotoxic effect and found evidence of a reduction in the Bcl-2 mRNA expression in MCF 7 breast cancer cell lines, which suggests promising anticancer effects (Selvanathan *et al.*, 2022).

Therefore, building on the established potency of ZnO NPs and the demonstrated bioactivity of *A. muricata* leaves, this study aims to synthesize biogenic ZnO NPs using *A. muricata* leaf extract to evaluate their antibacterial, antioxidant and photocatalytic activities. By utilizing the bioactive compounds from *A. muricata*, this biogenic synthesis approach offers a novel, environmentally sustainable alternative to chemically synthesized ZnONPs. The green synthesis of ZnONPs holds promise for various applications, from medical therapies to environmental remediation, with reduced ecological and cytotoxic risks.

MATERIALS AND METHODS

Materials
Ascorbic acid (Cipla, India), Ciprofloxacin (Sigma-Aldrich), Zinc nitrate hexahydrate (Sigma, Germany), 2-2-diphenyl-1-picrylhydrazl (DPPH) (Ranbaxy, India), methanol, petroleum ether (Ranbaxy, India), and ferric chloride (Sigma, Germany). The other reagents used were analytical grade.

Methods
Collection and preparation of A. muricata extract
Fresh *Annona muricata* leaves were obtained from Ibadan, Oyo State (Nigeria: 7° 22' 36.25" N and 3° 56' 23.23" E) in April 2023. Identifying and approving the authenticity of the leaves was conducted by Asst. Prof. Dr. Emmanuel Halilu of the Department of Pharmacognosy, Faculty of Pharmacy, Cyprus International University, Cyprus. A specimen voucher is kept with the Herbarium number CIU/PHARM/ ANNO/001 in Cyprus International University Public Herbarium. *A. muricata* leaves were washed adequately with deionized water, air dried and ground to powder using a mechanical blender. 10g of the ground powder was added to 100mL of methanol used as the solvent, which was then extracted by maceration for 72h at room temperature. Whatman No. 1 filter paper was used to filter the methanolic extracts and used immediately to synthesize ZnO nanoparticles. Additionally, crude extracts of *A. muricata* leaves were concentrated using a rotary evaporator (Heidolph HEI-VAP HL, Germany). Concentrated extracts were stored at 4°C until further use (Olasehinde *et al.*, 2022).

Synthesis of *A. muricata* zinc oxide nanoparticles
Zinc Oxide Nanoparticles (ZnO NPs) were prepared with/without the presence of *A. muricata* extracts, as previously described by Umar *et al.*, (2018). The plant

2

Pak. J. Pharm. Sci., Vol.38, No.2, March-April 2025, pp.001-012

extract was added to 0.1M concentrations of the zinc precursor at a ratio of 1:10 and stirred continuously at 500 rpm using a magnetic stirrer at 60ºC for 5h. 0.1 M of zinc nitrate hexahydrate (Zn (NO$_3$)$_2$.6H$_2$O) was prepared in 90 mL of distilled water; then, drop by drop, 10mL of *A. muricata* extract was added into the solution to synthesize the nanoparticles. The dropwise addition in a controlled manner ensures an adequate interaction between the biomolecules of AME and the zinc nitrate solution. A few drops of 2 M NaOH were added to maintain a pH of 12 as a high pH environment aid in forming a precipitate that facilitates the formation of the ZnO NPs. Blank zinc oxide nanoparticles were prepared as above without adding the plant extract and used as the control for the characterization of the synthesized nanoparticles. The samples were centrifuged to purify the zinc oxide nanoparticles at 4000 rpm for 20 min and repeated after re-washing using distilled water to eliminate any impurities. The supernatant was decanted, the residue of both the blank (zinc only) and mixture (zinc nitrate with extract complex) were dried in the oven at 50ºC to obtain dried fine, light cream ZnO powders, which were stored until further use (Abomuti *et al.*, 2021; Umar *et al.*, 2018).

Preliminary phytochemical analysis of AME
The preliminary phytochemical screening of AME was determined according to various identification tests to check for flavonoids, alkaloids, glycosides, tannins and saponins present as previously described by Halilu *et al.*, (2008).

Gas chromatography-mass spectrometry (GC-MS) analysis of AME
The qualitative phytochemical screening of AME was determined via GC-MS assay, as described by Shibula and Velavan. The study was performed in an Agilent 7890AGC system with an MS (Agilent Technologies) GCMS-QP2010 Plus System (Shimadzu, Japan). An HP-5 fused silica capillary column with 30 m x 0.25 mm (film thickness), 0.25μm was used. Helium was used with a 0.9mL/min flow rate. The oven temperature was programmed at 110°C for 2 min and then increased from 10°C/min to 200°C and finally at 280°C at 5°C/min for 10 min. The ion source was set at 280°C, while the injector temperature was 250°C with an injector volume of 0.5μL in split mode. The ionization of the sample parts was set to 70 eV. The mass spectra were recorded over the range of 50-550 m/z and compared against Wiley Library 7 and the NIST library were used to identify the compounds (Shibula and Velavan, 2015).

Analysis of total phenolic content (TPC)
The quantitative analysis of the total phenolic assay of AME was evaluated using the Folin-Ciocalteu reagent. 2.5mL of 10% Folin-Ciocalteu reagent (10%) with 2mL of sodium carbonate solution (2% w/v) was added to 0.5mL of AME solution (1mg/mL), The solution was incubated at room temperature for 15 min while shaking intermittently. Different concentrations of gallic acid solution (from 0 to 1mg/mL) were used to prepare a standard curve and a regression line. The resulting solution's absorbance was measured in triplicate through a UV-Vis spectrophotometer (Shimadzu UV-2450) at 765 nm (Aiyegoro and Okoh, 2010).

Estimation of total flavonoid content (TFC)
The total flavonoid assay of AME was performed using the Aluminum chloride colorimetric technique, as previously explained by Aiyegoro and Okoh (2010). Absorbance values were recorded at 420 nm with a UV-Vis spectrophotometer (Shimadzu UV-2450). A calibration curve was plotted having varying concentrations of gallic acid solution (from 0 to 1mg/mL) and a regression line was determined. The flavonoid concentration was expressed as mg gallic acid equivalents (GAE) per gram of dry extract (mg GAE/g) (Aiyegoro and Okoh, 2010).

Characterization of zinc oxide nanoparticles using Annona muricata extract
Characterization of *A. muricata* synthesized ZnO NPs was performed with the aid of various microscopic and spectroscopic techniques. The biosynthesized zinc oxide nanoparticles were confirmed with a UV-visible spectrophotometer (Shimadzu UV-2450) in the 200–800 nm range. Phase purity and crystalline structure of AME-ZnO NPs were analyzed using a Rigaku ZSX Primus II X-ray diffractometer (XRD, Rigaku, Japan). FTIR spectrophotometer (Shimadzu FT-IR Prestige-21 Model) was used to determine the Fourier transform infrared (FTIR) Spectra of AME-ZnO NPs between 400 to 4500cm^{-1}. The size distribution of the biosynthesized ZnO nanoparticles and the average diameter were analyzed using a laser particle size analyzer (Malvern Zeta sizer, UK). A Scanning Electron Microscope (SEM) (JEOL JSM-6701 F, Japan) was used to determine the morphological characteristics. The purity and primary composition of AME-ZnO NPs were observed using Energy-dispersive X-ray spectroscopy (EDX) (Oxford Instruments AZTEC EDS, USA) (Karthik *et al.*, 2023; Selvanathan *et al.*, 2022). The bandgap energy (E$_g$) can be determined from the UV-VIS absorption wavelengths by the Tauc plot using equation 1:

$$(\alpha h v)^n = A(h v - E_g) \tag{1}$$

Where α = absorption coefficient, hv = photon energy, E$_g$ = bandgap energy, and A is a constant.

Determination of the antibacterial activity of A. muricata synthesized zinc oxide nanoparticles
Five (5) bacterial species with three (3) gram-positive (Methicillin-resistant *Staphylococcus aureus* [Patient isolate donated by Dr. Burhan Nalbantoğlu Public Hospital], *Enterococcus faecalis* ATCC 29212, and *Bacillus subtilis* ATCC 6051), and two (2) gram-negative

(*Pseudomonas aeruginosa* ATCC 27853 and *Escherichia coli* O157:H7 (932)), obtained from the Microbiology Laboratory, Cyprus International University, were grown at 37°C at relative humidity.

Minimum inhibitory concentration (MIC)
The minimum inhibitory concentration (MIC) assay was prepared via the broth dilution method using 96-well microtiter plates (Thermo Scientific™). Fresh broth cultures of 5 bacterial species were standardized to 0.5 McFarland. A 10mg/mL stock solution of AME and AME-ZnO NPs was prepared and subjected to a 2-fold serial dilution directly in the well plates, starting from 10 mg/ml down to 0.0195mg/mL. A spectrophotometer (EL*x*800) observed the turbidity of the micro plates at 600 nm after incubation overnight at 37°C. The tests were performed three times in triplicates and t-test was used to compare the bacterial growth at various concentrations to determine the MIC based on statistically significant (p<0.05) difference when compared to the control. (Kowalska-Krochmal and Dudek-Wicher, 2021). Negative control wells only received Muller Hinton broth, while positive control wells received Ciprofloxacin antibiotic (Sigma-Aldrich HPLC grade).

Antioxidant activity using 2,2-diphenylpicrylhydrazyl (DPPH) radical scavenging assay
The anti-oxidation activity of *A. muricata* ZnO NPs was performed via the modified method by Xiao *et al.*, (2020). A two-fold dilution was used to prepare graded concentrations of the samples. Briefly, 1.5mL of 0.1mM solution of DPPH in methanol solvent was added to 1.5mL of the samples, and the samples were allowed to incubate in the dark for 60 minutes at room temperature. The absorbance was read at 517 nm via a UV-VIS spectrophotometer (Shimadzu UV-2450). The scavenging activity of DPPH radical was calculated in equation 2 as:

$$\% \text{Inhibition} = (\frac{1-(A_1 - A_2)}{A_o} \times 100 \qquad (2)$$

Where A_0 is the absorbance of the control (without sample), A_1 is the absorbance of the sample and A_2 is the absorbance of the blank sample (without DPPH radical). (Sasikumar and Pavithra, 2021).

Determination of photocatalysis degradation assay
The photocatalytic assay, as explained by Nguyen *et al* was utilized to assess the degradation efficiency of *A. muricata* ZnO NPs on methylene blue (MB) dye. The analysis was conducted using ultraviolet irradiation by placing the samples in a UV-Vis lightbox. A 5 ppm MB dye solution was prepared and agitated without light for 1 hour to allow it to attain adsorption-desorption equilibrium. From the 5 ppm MB dye solution, 50mL of the solution was taken, and 20 mg of the AME-ZnO NPs was added to it and placed on an Ultrasonicator. 4 of the samples were prepared and sonicated at different mixing times of 15-, 30-, 45- and 60 min. After sonication, the mixture was placed in the UV-Vis light box for 180 min.

During this time, 5mL was aliquoted every 30 min and centrifuged and the absorbance values were recorded at a wavelength of 665 nm. The degree at which the MB dye was degraded during treatment was calculated by comparing its absorbance after treatment with its initial absorbance and expressed as a percentage reduction (Nguyen *et al.*, 2023).

STATISTICAL ANALYSIS

Statistical analysis was evaluated via the student's unpaired *t-test* using Origin Pro (version 2021) and Graph Pad Prism software (version 8.0.2). Data were expressed as mean ± SEM. All the experiments were performed three times in triplicates (n≥3). p<0.05 were considered significant.

RESULTS

The phytochemical composition of A. muricata extract
The phytochemical composition of the *A. muricata* extract (table 1) indicated secondary metabolites like flavonoids, saponins and tannins that can be found in the plant extract.

Chemical composition of A muricata extract
Gas Chromatography-Mass Spectrophotometry (GC-MS) has been utilized for bio-constituent examination of the methanolic leaf extract of *A. muricata*. The results (fig. 1, table 2) with the retention time (Ret. Time), molecular formula and the nature of the compounds revealed that the *A. muricata* leaf extracts include several bioactive constituents with various biological activities.

Total phenolic assay (TPA)
Annona muricata leaf extract was found to have a total phenolic content of 0.081±0.001mg/g Gallic acid equivalent (GAE/) with reference to the standard curve (fig. 2).

Total flavonoid content (TFC)
The total flavonoid assay revealed a value of 0.987 ± 0.039 mg Gallic acid equivalent per gram of extract powder.

UV-VIS spectrum analysis
UV-VIS spectrophotometry analysis was performed to verify the AME-ZnO NPs present in its colloidal solution. The optical property of the peak showed an absorption band at 370 nm (fig. 3a), while the observed bandgap energy of the AME-ZnO NPs was 3.11 eV (fig. 3b), therefore confirming the successful synthesis of the nanoparticles.

Fourier transform infrared spectroscopy (FTIR) spectrum of AME-ZnO nanoparticles.
The result of the FTIR spectra (fig. 4) performed on the *A. muricata* synthesized ZnO nanoparticles revealed

Table 1: Phytochemical screening of the methanolic leaf extract of *A. muricata* indicated the presence of flavonoids, alkaloids, phenolic compounds, tannins, and saponins.

	Name of Test		Observation	Results
1.	Flavonoids	Alkaline Reagent test	Yellow color formation	+
2.	Alkaloids	Dragendroff's test	Orange precipitate	+
		Mayer's test	Orange precipitate	+
3.	Phenols	Ferric chloride test	Dark green precipitate	+
4.	Tannins	Ferric chloride test	Blue-black precipitate	+
5.	Saponins	Frothing Test	Persistent frothing	+

+ = present

Table 2: Most abundant phytochemical bioactive molecules of the methanolic leaf extract of *A. muricata* by Gas Chromatography-Mass Spectrophotometry (GC-MS) analysis.

S N	Compound detected	R. Time	Molecular Formula	Nature of compound
1	Bis[3-(2-methoxy-ethoxy)methoxy]-11-iodo-9,11-seco-C-nor-5.beta.-yl Formates	1.434	$C_{29}H_{54}O_8$	Acetogenins
2	trans-Caryophyllene	7.670	$C_{15}H_{24}$	Sesquiterpenes
3	Germacrene D	11.927	$C_{15}H_{24}$	Sesquiterpenes
4	Linoleic acid	18.934	$C_{18}H_{32}O_2$	Fatty acids
5	Octadecanoic acid, methyl ester	23.329	$C_{19}H_{38}O_2$	Fatty acids
6	Geraniol	25.214	$C_{10}H_{18}O$	Terpenoid
7	n-Dotriacontanoic acid	26.032	$C_{32}H_{64}O_2$	Fatty acids
8	eicosanoic acid	29.758	$C_{20}H_{40}O$	Fatty acid
9	Ceanothine C	30.005	$C_{26}H_{38}N_4O_4$	Alkaloids
10	Eicosanoic acid	30.618	$C_{20}H_{40}O_2$	Fatty acids
11	Pristane 2,6,10,14-tetramethylpentadecane	30.878	$C_{19}H_{40}$	Hydrocarbon
12	Cantharidin	30.933	$C_{10}H_{12}O_4$	Terpenoid
13	9-[2'-Deoxy-3',5'-ethano-.beta.-D-ribofuranosyl]thymine	32.267	$C_{12}H_{16}N_2O_5$	Nucleoside
14	Clemastin	32.425	$C_{21}H_{26}ClNO$	Antihistamines
15	Oleic acid	33.021	$C_{18}H_{34}O_2$	Fatty acids
16	3-acetyl-2-oxo-4-hydroxy-5-methylpyrrolidine	33.925	C8H11NO3.	Pyrrolidines
17	(2S) -2-methyl-4- [(2R,8R,13R) -2,8,13-trihydroxy-13-[(2R,5R)-5-[(1R)-1-hydroxytridecyl]oxolan-2-yl]tridecyl]- 2H-furan-5-one	34.275	$C_{35}H_{64}O_7$	Acetogenins
18	Annonacin	34.884	$C_{35}H_{64}O_7$	Acetogenins
19	n-Hexadecanoic acid	35.683	$C_{16}H_{32}O_2$	Fatty acids
20	Goniothalamicin	36.980	$C_{35}H_{64}O_7$	Acetogenins

Table 3: Minimum inhibitory concentrations (MIC) of *Annona muricata* leaf extracts and the synthesized ZnO nanoparticles against tested bacterial strains *Staphylococcus aureus* (MRSA), *Enterococci faecalis* ATCC 29212, *Bacillus subtilis* ATCC 6051, *Pseudomonas aeruginosa* ATCC 27853, *Escherichia coli* O157: H7 (932). Data is expressed as the mean ± SEM (n = 3).

	Gram-positive		Gram-negative		
	Staphylococcus aureus (MRSA)	*Enterococci faecalis* ATCC 29212	*Bacillus subtilis* ATCC 6051	*Pseudomonas aeruginosa* ATCC 27853	*Escherichia coli* O157:H7 (932)
AME (mg/mL)	2.5±0	1.25±0	1.25±0	5±0	5±0
AME-ZnONPs (mg/mL)	0.63±0	0.63±0	0.32±0	1.25±0	2.5±0
Ciprofloxacin (mg/mL)	0.32±0	0.15±0	0.15±0	0.63±0	0.32±0

characteristic spectral bands such as 3450cm⁻¹, 2160cm⁻¹ and 1940cm⁻¹ aligned with an elongated O-H polyphenols bond and demonstrated C-O bond stretch of flavonoids. The indicated peak at 1635cm⁻¹ corresponds with the absorbed H-O-H molecule's bending vibration. The absorption peak at 1448cm⁻¹ for the AME-ZnO NPs is assigned to the C-N bond, indicating alkaloids from the AME, while the absorption band at 1056 cm⁻¹ is assigned to the intermolecular stretching of the 0-H bond and stretching of the C=O and C-C functional group. The spectrum shows an absorption peak at 835 cm⁻¹ corresponding to Zn-O-H stretching peaks and also corresponds to the C–H out-of-plane bending vibrations of aromatic groups or phenolic compounds such as alkaloids. The peak observed at 648 cm⁻¹ corresponds to the Zn-O bond's stretching frequency, indicating the bond's vibrational band.
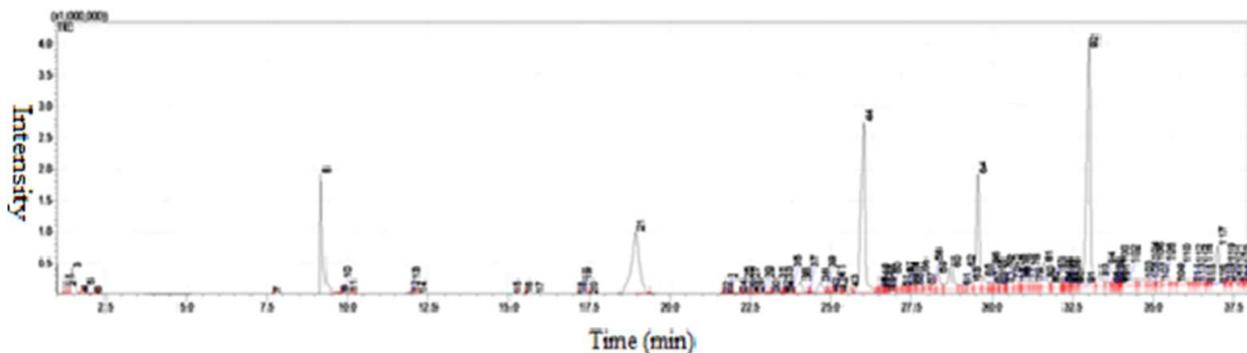
Pak. J. Pharm. Sci., Vol.38, No.2, March-April 2025, pp.001-012

5

Fig. 1: Gas Chromatography-Mass Spectrophotometry (GC-MS) chromatogram from the *Annona muricata* leaf methanolic extract. The peak numbers are corresponding to the bioactive molecules stated in table 2.

Particle size distribution of synthesized nanoparticles

The particle size of the AME-ZnO NPs was analyzed using a laser particle size analyzer (Malvern Zeta Sizer, UK) using the dynamic light scattering (DLS) technique. The biosynthesized nanoparticles were found to have a relatively uniform size distribution, which was revealed with a polydispersity index of 0.2363 and an average particle size of 79.14 ± 2.0 nm (fig. 5b), which was higher than the blank zinc nanoparticle presenting an average size of 59.5 ± 0.8 nm (fig. 5a).

Scanning electron microscopy and EDX analysis

Scanning Electron Microscopy (SEM) was performed to examine the morphology of AME-ZnO NPs. The images reveal a quasi-spherical shape, and the particles are in a highly agglomerated form compared to the blank zinc nanoparticles (fig. 6a & fig. 6b). The EDX of the NPs reveals that the zinc oxide nanoparticles majorly contain 82.79% zinc (Zn) and 17.21% oxygen (O) (fig. 7).

XRD Analysis

The AME-ZnO nanoparticles XRD pattern indicates a significant widening of the XRD peaks, which implies that the diameters of the particles under synthesis are in the nanometer range (fig. 8).

Determination of minimum inhibitory concentration (MIC) of AME-ZnO NPs against pathogenic bacteria

The minimum inhibitory concentration assay was performed to determine antimicrobial effects of AMEs, AME-ZnO NPs. Ciprofloxacin was used as positive control. MIC experiment results revealed that both the nanoparticles and the plant extract demonstrated significant antimicrobial effects against *Staphylococcus aureus* (MRSA), *Enterococci faecalis* ATCC 29212, *Bacillus subtilis* ATCC 6051, *Pseudomonas aeruginosa* ATCC 27853, *Escherichia coli* O157:H7 (932). MIC values were obtained at the specified concentrations in table 3, indicating that bacterial growth was effectively inhibited at these levels.

Determination of total antioxidant activity

A DPPH assay was used to analyze the antioxidant effect of A. muricata extract and the synthesized ZnO NPs were synthesized *in vitro*. Ascorbic acid was used as positive control. AME-ZnO NPs demonstrated a free radical scavenging activity with an IC_{50} of 1.66 mg/mL, which is higher than the IC_{50} of the extract, which was 2.17mg/mL. Ascorbic acid exhibited a higher radical scavenging activity than the extract and ZnO NPs with an IC_{50} of 0.23mg/mL and the highest percentage inhibitions values of 99.43 ± 0.09 at 10mg/mL. At 10 mg/mL concentration, AME-ZnO NPs exhibited higher activity when compared with the AME, with percentage inhibition values of 89.61 ± 0.64 and 76.75 ± 0.89, respectively (fig. 9).
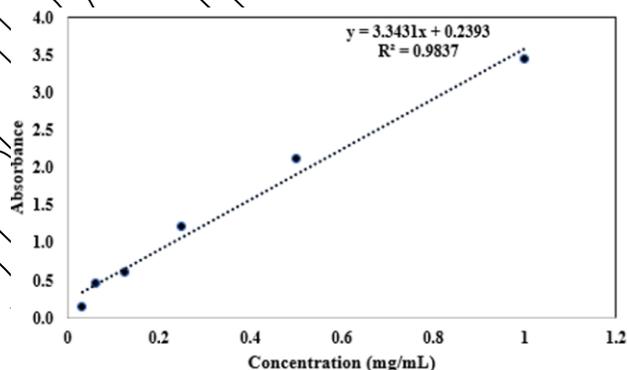

Fig. 2: Calibration curve of standard gallic acid for determining total phenol content in *Annona muricata* leaf extract.

Photocatalytic degradation

An increase in photocatalytic degradation was observed after prolonged mixing and exposure to UV light (fig. 10). Extending the irradiation time leads to a higher percentage degradation of methylene blue, which is indicated by a decrease in the absorption peak intensity at 665 nm. At a mixing time of 60 min, there was a higher degradation efficiency compared to the lower mixing time, showing that higher contact time aids the degree of degradation. The biosynthesized ZnO NPs expressed a higher MB dye decomposition at 60% after 180 min of UV light exposure at a value of 67.44 % when compared to the 45-, 30- and 15-min mixing time with the maximum degradation percentage values of 59.52, 51.12, and 47.47 respectively.
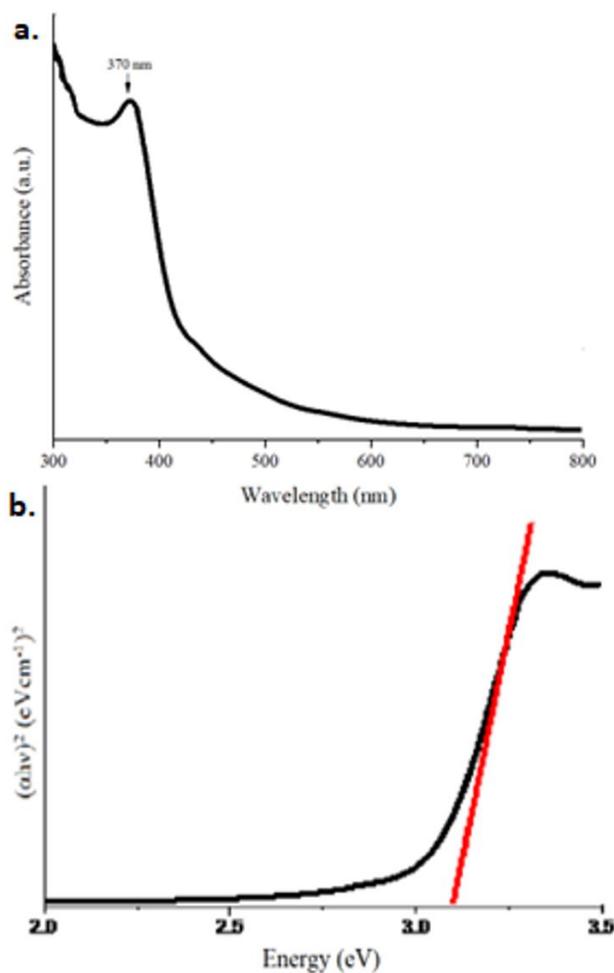
Fig. 3: UV-VIS spectra showing a characteristic peak of ZnO NP at 370 nm (a) and Tauc plot of AME-ZnO NPs showing a 3.11 eV bandgap energy (b) confirms the successful synthesis of the nanoparticles.
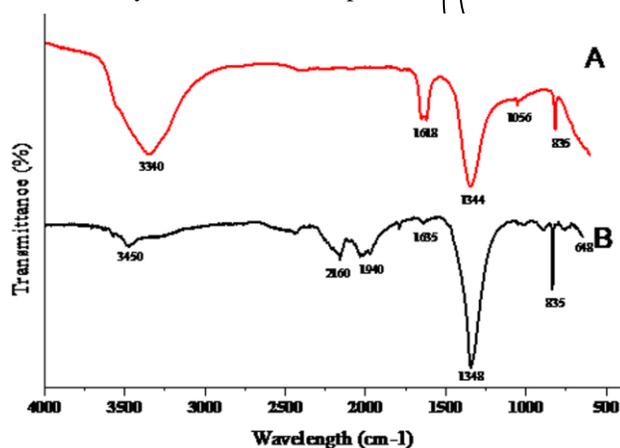

Fig. 4: Fourier transform infrared spectrum (FTIR) of the blank ZnONPs (A) and the ZnO NPs using *A. muricata* leaf extract (B). The prominent peaks in the AME-ZnO NPs indicate the bioactive functional groups present, which suggest the successful capping of ZnO

nanoparticles by the phytochemicals in *A. muricata*, leading to enhanced stabilization.
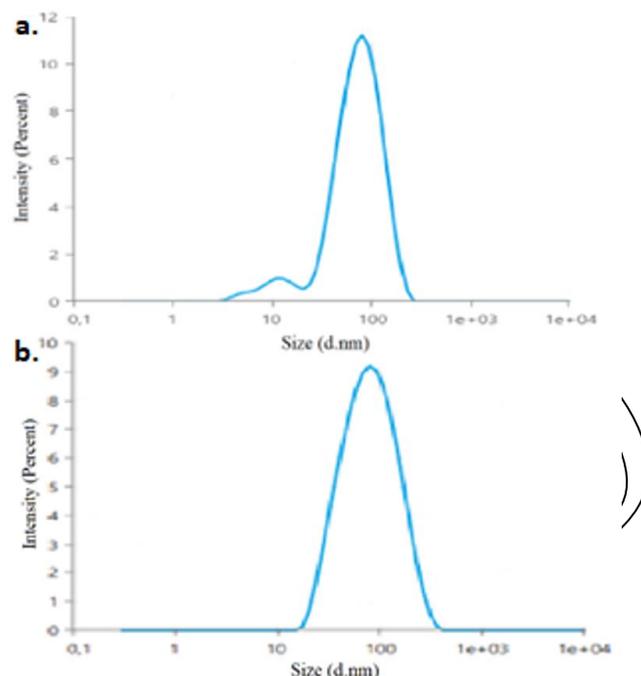
Fig. 5: Dynamic light scattering (DLS) analysis showing the particle size distribution of (a) blank ZnO nanoparticles and (b) biosynthesized ZnO nanoparticles using *Annona muricata* leaf extract (AME-ZnO NPs). The blank ZnO NPs reveal a smaller average particle size of 59.5±0.8 nm, whereas the AME-ZnO NPs have a larger average size of 79.14±2.0 nm, with a polydispersity index (PDI) of 0.2363, indicating a relatively uniform size distribution.

DISCUSSION

Phytochemical molecules such as alkaloids, flavonoids, acetogenins, saponins and tannins, as well as some vitamins and reducing sugars present in *A. muricata,* were shown to aid in the reduction and stability of biosynthesized zinc oxide nanoparticles (ZnO NPs). The GC-MS analysis identified compounds such as terpenoids and sesquiterpenes in AME, which likely contribute to the antimicrobial activities, while flavonoids and acetogenins aid in the antioxidation and photocatalytic effects (Vidhya *et al*., 2023; Lih *et al.,* 2024).

Observation of the optical property using the UV-VIS spectrophotometry, showed a characteristic absorption peak between 350 and 450 nm, which indicates the crystalline nature of the nanoparticles. The obtained result corresponds with previous studies showing similar wavelengths around 370 nm and also aligns with prior studies having a wide bandgap caused by their small particle size (Mallikarjunaswamy *et al.*, 2020, Yassin *et al.,* (2022). FTIR analysis of AME-ZnONPs confirmed

the functional groups involved in the reduction and stabilization of the nanoparticles. Peaks observed at 2160 cm^{-1} and 1940 cm^{-1} corresponded to biomolecules in *A. muricata* acting as reducing and capping agents, consistent with studies on plant-based nanoparticle synthesis (Sivaranjani and Meenakshisundaram, 2022; Bhattacharjee *et al*., 2024). The presence of C-N bonds between 1400-1600cm^{-1} indicated alkaloids, essential for nanoparticle stability (Sharma *et al*., 2022). Additionally, the peak at 835 cm^{-1}, linked to out-of-plane bending vibrations of aromatic C-H bonds, likely corresponds to phenolic compounds and flavonoids aiding in nanoparticle formation (Yassin *et al*., 2023; Dash *et al*., 2021). The Zn-O bond stretch at 835cm^{-1}, observed in both blank and AME-ZnONPs, further confirmed the characteristic ZnO lattice, supporting findings from previous studies on zinc oxide nanoparticles (Nguyen *et al*., 2023; Davis *et al*., 2019).
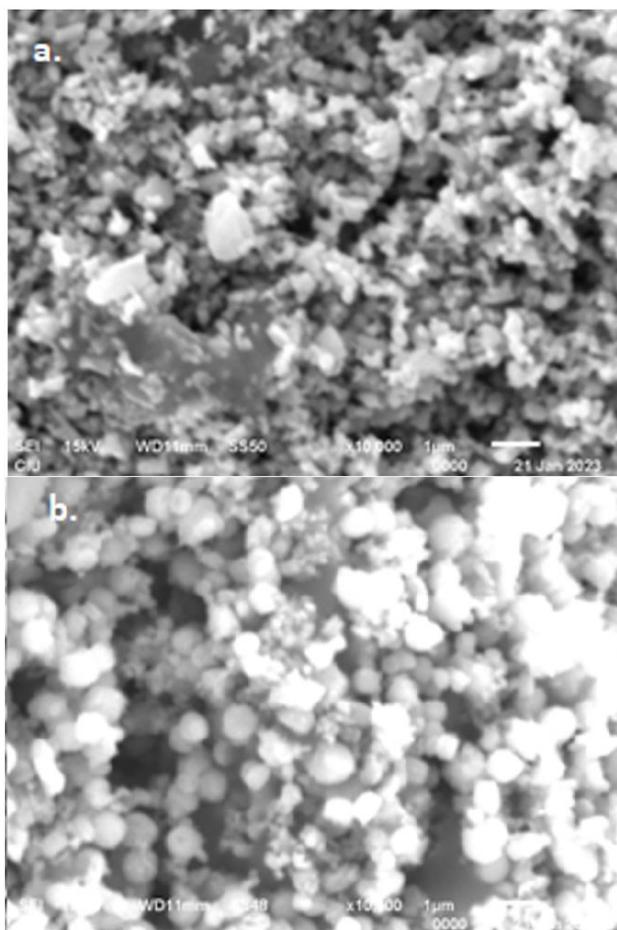
capping agents, which enhances nanoparticle formation and prevents excessive clustering, leading to nanoparticles with potential for improved bioactivity and stability.
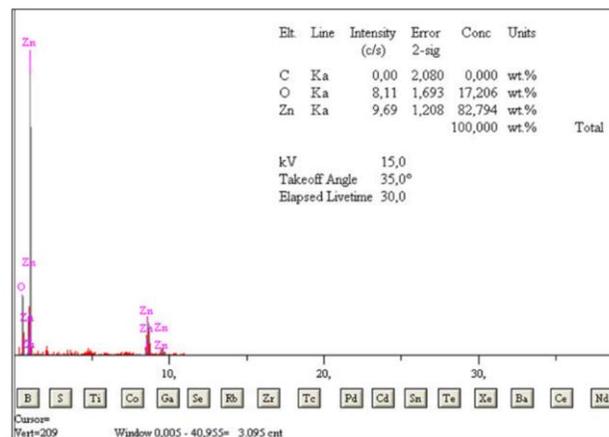

Fig. 7: Energy Dispersive X-ray spectroscopy (EDX) of the biosynthesized ZnONPs using *A. muricata* leaf extract where the elemental composition and weight % were confirmed.
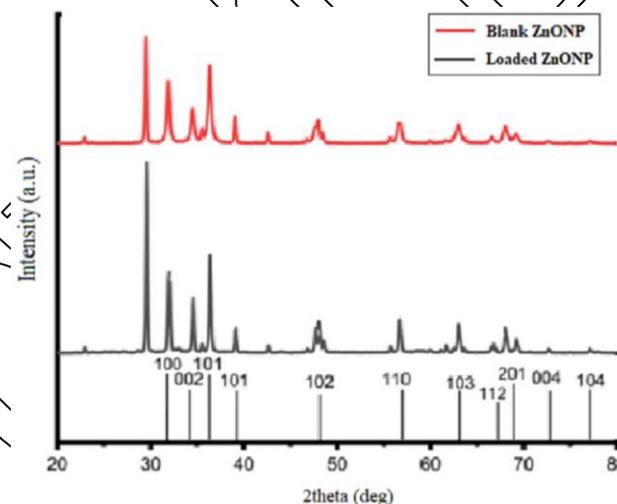

Fig. 8: X-ray diffraction (XRD) spectra of blank ZnO nanoparticles (red) and ZnO nanoparticles synthesized using *Annona muricata* leaf extract (black) reveal sharp diffraction peaks indicative of ZnO's hexagonal wurtzite structure. Prominent peaks at 31.60°, 34.54° and 36.16° correspond to the (100), (002) and (101) planes, respectively. The similarity in both spectra confirms the crystalline structure of the ZnO nanoparticles in each sample.

Fig. 6: Scanning electron microscopy (SEM) images of the blank ZnO NPs (a) and the zinc oxide nanoparticles using *A. muricata* leaf extract (b). The blank ZnO NPs display irregularly shaped agglomerates, while the AME-ZnO NPs exhibit a more uniform, spherical morphology with less agglomeration. The improved particle dispersion in the AME-ZnO NPs suggests that the bioactive compounds from *A. muricata* act as stabilizing and

Incorporating *A. muricata* extract in ZnO NP synthesis resulted in increased particle size and stability, as evidenced by SEM and PDI analysis. The low polydispersity index indicates homogeneity and uniformity of the particles, which is essential for applications in drug delivery and biotechnology. SEM images revealed particle aggregation due to overlapping

particles, consistent with studies on other plant-extract-mediated ZnONPs (Karthik *et al*., 2023; Vignesh *et al.,* 2022). EDX analysis further confirmed the purity of the synthesized nanoparticles and XRD results showed high crystallinity with peaks that matched the hexagonal wurtzite phase of ZnO, similar to those reported in recent studies (Gupta *et al*., 2021). The crystallinity of AME-ZnONPs, enhanced by calcination, was attributed to the releasing gases during synthesis, which helped purify the nanoparticles and eliminate impurities. The sharp, narrow diffraction peaks observed in the XRD analysis support the high-quality crystalline structure of the nanoparticles, as also noted by Karthik *et al*. (2023) and Karkhane *et al*. (2020). Recent studies also show prominent diffraction peaks highlighting the consistency among plant-mediated ZnONPs (Lakshmeesha *et al*., 2023).
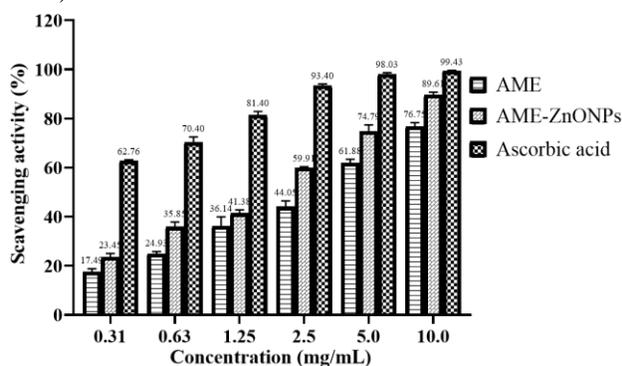
Fig. 9: 2,2-diphenyl-1-picrylhydrazyl (DPPH) Radical Scavenging Assay of *Annona muricata* leaf extract (AME), AME-ZnO Nanoparticles (AME-ZnONPs), and ascorbic acid. Data represented as ± SEM (n=3). Ascorbic acid exhibited the highest scavenging activity across all concentrations, where, AME-ZnONPs exhibited significantly higher antioxidant potential compared to AME alone, especially at higher concentrations (96.53% at 10.0mg/mL). These results indicate that the incorporation of ZnO nanoparticles enhances the antioxidant properties of *A. muricata* extract, likely due to synergistic effects between the bioactive compounds in the plant and the nanoparticles.

The antimicrobial efficacy of AME and AME-ZnO NPs had enhanced efficacy across multiple bacterial strains and showed distinctly lower MIC values for AME-ZnO NPs compared to AME alone. The MIC results suggest a synergistic effect between ZnO and the bioactive compounds in *A. muricata*, which enhances antibacterial potency. Similar studies have demonstrated comparable improvements in antibacterial activity when metal nanoparticles are combined with plant extracts, with MIC values in the same range (Bhattacharjee *et al*., 2024; Murali *et al*., 2021). The enhanced antimicrobial mechanism of AME-ZnO NPs is likely due to the generation of reactive oxygen species (ROS), causing oxidative stress and membrane disruption in bacterial

cells, similar to findings in other metal-based nanoparticle studies (Nguyen *et al*., 2023).
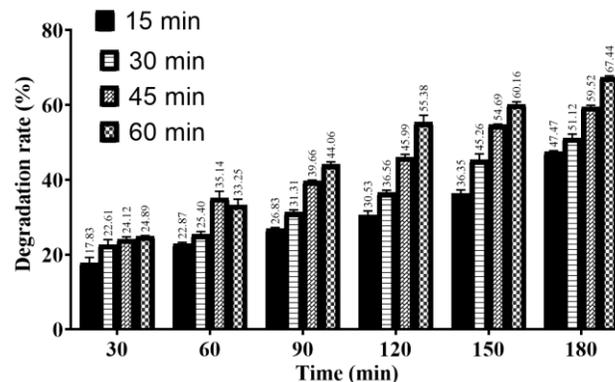
Fig. 10: Photocatalytic activity of AME-ZnO NPs in degrading methylene blue under different time intervals and light exposure durations under various time intervals (30, 60, 90, 120, 150 and 180 minutes). The data show that the degradation rate increases with longer exposure times, peaking at 64.44% after 180 minutes with 60 minutes of light exposure. These findings highlight the significance of reaction time and light exposure in optimizing the degradation efficiency of pollutants using ZnO nanoparticles synthesized with *A. muricata* extract. Data represented as ± SEM (n=3).

DPPH assay demonstrated significant free radical scavenging activity across all concentrations, where higher concentrations yield greater antioxidant activity due to the increased number of active sites available for interaction with DPPH radicals (Mendes *et al*., 2022). The synthesized ZnO nanoparticles using *A. muricata* leaf extract (AME-ZnO NPs) acted as effective hydrogen or electron donors, neutralizing the radicals and preventing oxidative damage. While our reported IC_{50} value of 1.66 mg/mL may seem higher than conventional antioxidants, it is consistent with findings from other studies involving metal nanoparticles, which often require higher concentrations for optimal activity (Nguyen *et al*., 2023; Bhattacharjee *et al*., 2024; Halilu *et al*., 2024). This is due to the larger surface area of nanoparticles, allowing for a more pronounced dose-response relationship in antioxidant assays. Additionally, the acetogenins, flavonoids, and other bioactive compounds in *A. muricata* have been shown to contribute to its antioxidant activity (Karthik *et al*., 2023). The functional groups on the AME-ZnO NPs likely facilitate direct interaction with DPPH radicals, enhancing their radical scavenging efficiency (Nguyen *et al*., 2023). Thus, the higher IC_{50} value in this study is justified by the nature of metal nanoparticles and aligns with the antioxidant activity observed in other green-synthesized nanoparticles.

Photocatalytic activity of the AME-ZnO NPs can be attributed to ZnO nanoparticles' ability to generate reactive species such as hydroxyl (OH) and superoxide

(O_2^-) radicals under UV irradiation, which causes a breakdown of methylene blue into CO_2 and H_2O (Bhattacharjee *et al*., 2024). The ZnO NPs' wide band gap of 3.11 eV supports their ability to absorb UV light and efficiently drive electron-hole pair formation, facilitating pollutant degradation (Ogbonna and Kavaz, 2024). These findings align with previous studies, that reported similar efficacies for ZnO nanoparticles in photocatalytic degradation, highlighting their potential for environmental remediation applications (Tegenaw *et al*., 2023; Cao *et al*., 2019).

Combining the effectiveness of ZnO nanoparticles' antimicrobial action with its photocatalytic ability creates a dual-action material, as the reactive oxygen species (ROS) generated upon exposure to light causes damage to bacterial cell walls and membrane, thereby hindering the growth of microorganisms (Rajalakshmi *et al.,* 2023).

CONCLUSION

In this study, we demonstrated the synthesis of ZnO nanoparticles using *Annona muricata* leaf extract through an eco-friendly green synthesis method that exhibited significant antibacterial, antioxidant and photocatalytic properties. However, further research is necessary to evaluate their biocompatibility and toxicity, particularly through *in vivo* studies, to confirm their safety for biomedical applications. Assessing their cytotoxic effects and long-term environmental impact will be crucial for ensuring their safe use in both therapeutic and environmental contexts. Future studies in these areas will be key to unlocking the full potential of AME-ZnO NPs for clinical and ecological applications.

REFERENCES

Abomuti MA, Danish EY, Firoz A, Hasan N and Malik MA (2021). Green synthesis of Zinc oxide Nanoparticles using *Salvia officinalis* leaf extract and their photocatalytic and antifungal activities. *Bio Nano Sci.,* **10**(11): 1075-1082.

Afroz N, Hoq MA, Jahan S, Islam MM, Ahmed F, Shahid-Ud-Daula AFM and Hasanuzzaman M (2020). Methanol soluble fraction of fruits of *Annona muricata* possesses significant antidiarrheal activities. *Heliyon.,* **6**(1): e03112.

Ahmed WM, Ibrahim IA, Ibrahim AA and Alsemeh AIM (2023). Possible toxicological effects of zinc oxide nanoparticles on lungs. *Tob. Regul. Sci.,* **9**(1): 158-161.

Aiyegoro OA and Okoh AI (2010). Preliminary phytochemical screening and *in vitro* antioxidant activities of the aqueous extract of *Helichrysum longifolium* DC. *BMC Complement. Altern. Med.,* **10**(1): 21-30.

Bhattacharjee N, Som I, Saha R and Mondal S (2024). A critical review on novel eco-friendly green approach to synthesize zinc oxide nanoparticles for photocatalytic degradation of water pollutants. *Int. J. Env. Anal. Chem.*, **104**(3): 489-516.

Cao F, Wang T and Ji X (2019). Enhanced visible photocatalytic activity of tree-like ZnO/CuO nanostructure on Cu foam. *Appl Surf Sci.*, **471**: 417-424.

Dash GK, Bin Hashim MH, Russ Hassan AK and Muthukumarasamy R (2021). Pharmacognostic Studies on the leaves of *Annona muricata* Linn. *Pharm. J.*, **13**(1): 241-247.

Davis R, Patel T and Singh K (2019). Spectroscopic analysis of ZnO nanoparticles and their environmental impact. *Environ. Nanotechnol.*, **15**(2): 85-94.

Dias DA, Urban S and Roessner U (2012). A Historical overview of natural products in drug discovery. *Metabolites*, **2**(2): 303-336.

Fujihara J and Nishimoto N (2024). Review of Zinc Oxide Nanoparticles: Toxicokinetics, Tissue Distribution for Various Exposure Routes, Toxicological Effects, Toxicity Mechanism in Mammals, and an Approach for Toxicity Reduction. *Biol. Trace Elem. Res.*, **202**(1): 9-23.

Gupta R, Singh M and Joshi K (2021). Characterization and photocatalytic activity of plant-mediated ZnO nanoparticles. *RSC Advances*, **11**(34): 20400-20410.

Halilu EM, Airemwen CO and Omolan E (2024). Antibacterial and antioxidant studies of silver nanoparticles formulated from *Erythrina senegalensis* stem bark extract. *Pak. J. Pharm. Sci.*, **37**(4): 891-901

Halilu ME, Akpulu IK, Agunu A, Ahmed A and Abdurahman (2008). Phytochemical and Antibacterial Evaluation of Parinari curatetellifolia Planch Ex Benth (Chrysobalanaceae). *Nig. J. Bas. and App. Sci.*, **16**(2): 281-285.

Karkhane M, Yazdanpanah A, Tavakoli R and Hadian-Ghazvini S (2020). X-ray diffraction and morphological analysis of green-synthesized ZnO nanoparticles using plant extract. *Pak. J. Pharm. Sci.*, **33**(5): 1203-1210.

Karthik M, Ragunath C, Krishnasamy P, Queen Paulraj D and Ramasubramanian V (2023). Green synthesis of zinc oxide nanoparticles using *Annona muricata* leaf extract and its antioxidant and antibacterial activity. *Inorg. Chem. Commun.*, **157**(2): 1-9.

Kowalska-Krochmal B and Dudek-Wicher R (2021). The Minimum Inhibitory Concentration of Antibiotics: Methods, Interpretation, Clinical Relevance. *Pathogens*, **10**(2): 165-173.

Kumaran A, Sundari T and Patel RK (2021). Phytotherapeutic applications of Annona muricata: Insights into its ethnobotany and pharmacology. *Phytother Res.*, **35**(4): 789-799.

Lakshmeesha TR, Niranjana SR and Prasad K (2023). Green synthesis and characterization of ZnO nanoparticles using Cinnamomum verum bark extract

and their antibacterial properties. *Biomolecules*, **10**(2): 336-340.

Lih HT, Airemwen CO and Halilu EM (2024). Phytochemical Studies and Evaluation of Silver Nanoparticles Synthesized from *Solanum elaeagnifolium* Leaves Extract for Antioxidant and Antibacterial Activities. *Trop. J. Nat. Prod. Res.*, **8**(2): 6440-6445.

Mallikarjunaswamy C, Lakshmi Ranganatha V, Ramu R, Udayabhanu and Nagaraju G (2020). Facile microwave-assisted green synthesis of ZnO nanoparticles: Application to photodegradation, antibacterial and antioxidant. *J. Mater. Sci. Mater. Electron.,* **31**(2): 1004-1021.

Mendes CR, Dilarri G, Forsan CF, de Sapata V, Lopes PRM, de Moraes PB and Bidoia ED (2022). Antibacterial action and target mechanisms of zinc oxide nanoparticles against bacterial pathogens. *Sci Rep*., **12**: 1-10.

Monfared V, Salehian A, Nikniaz Z, Ebrahimpour-Koujan S and Faghfoori Z (2023). The effect of zinc supplementation on anthropometric measurements in healthy children over two years: A systematic review and meta-analysis. *BMC Ped*., **23**(1): 414-420.

Muhtadi M, Mugiyanto E, Nizmah Fajriyah N, Slamet S, Waznah U, Bagus Pambudi D, Fridiana, Safitri ED and Rosyid FN (2023). Formulation and evaluation of topical nano-hydrogel of Zinc and Annona Muricata extract. *Ind. J. Pharm.,* **34**(2): 291-301.

Murali M, Kalegowda N, Gowtham HG, Ansari MA, Alomary MN, Alghamdi S, Shilpa N, Singh SB, Thriveni MC, Aiyaz M and Angaswamy N (2021). Plant-Mediated Zinc Oxide Nanoparticles: Advances in the New Millennium towards Understanding Their Therapeutic Role in Biomedical Applications. *Pharmaceutics*., **13**(10): 1662.

Mutakin M, Fauziati R, Fadhilah FN, Zuhrotun A, Amalia R and Hadisaputri YE (2022). Pharmacological activities of soursop (*Annona muricata* Linn). *Molecules*, **27**(4): 1201-1211.

Nguyen TTT, Nguyen YNN, Tran XT, Nguyen TTT and Van TT (2023). Green synthesis of CuO, ZnO and CuO/ZnO nanoparticles using *Annona glabra* leaf extract for antioxidant, antibacterial and photocatalytic activities. *J Environ Chem Eng*. **11**(5): 111-119.

Ogbonna C and Kavaz D (2024). Green synthesis of hybrids of zinc oxide, titanium oxide, and calcium oxide nanoparticles from *Foeniculum vulgare*: An assessment of biological activity. *Chem Eng Commun*., **211**(7): 1072-1098.

Olasehinde OR, Afolabi OB, Owolabi OV, Akawa AB and Omiyale OB (2022). GC-MS analysis of phytochemical constituents of methanolic fraction of *Annona muricata* leaf and its inhibition against two key enzymes linked to type II diabetes. *Sci Afr.*, **16**(3): 01178-1185.

Rajalakshmi R, Doss A, Rani TPKP, Manikandan B, Rajeswari G and Aranganayaki J (2023). Eco-friendly synthesized zinc oxide nanoparticles an antibacterial agent. *Biomass Conv. Bioref*., **6**(2): 1-14.

Reid BJ, Palmer H, Barber SA and Crossley J (2023). Advances in green synthesis of nanoparticles: addressing environmental impacts and therapeutic potential. *J. Appl. Nanosci.,* **45**(2): 178-189.

Reid M, Whatley V, Spooner E, Nevill AM, Cooper M, Ramsden JJ and Dancer SJ (2018). How Does a Photocatalytic Antimicrobial Coating Affect Environmental Bioburden in Hospitals? *Infect Control Hosp Epidemiol.*, **39**(4): 398-404.

Sasikumar P and Pavithra S (2021). Evaluation of Antioxidant Activity Using DPPH Assay in Nanoparticle Applications. *J. Phytochem. Nanobiotechnol*, **8**(4): 223-231.

Selvanathan V, Aminuzzaman M, Tan LX, Win YF, Cheah ES, Heng MH, Tey LH, Arullappan S, Algethami N, Alharthi SS and Sultana S (2022). Synthesis, characterization and preliminary *in vitro* antibacterial evaluation of ZnO nanoparticles derived from soursop (*Annona muricata* L.) leaf extract as a green reducing agent. *J. Mater. Res. Technol.*, **20**(2): 2931-2941.

Sen T and Samanta SK (2014). Medicinal plants, human health and biodiversity: A broad review. In: Mukherjee J editors. *Biotechnol. Appl. Biodivers.*, 1st ed., Springer, New York: 59-110.

Sharma P, Urfan M, Anand R, Sangral M, Hakla HR, Sharma S, Das R, Pal S and Bhagat M (2022). Green synthesis of zinc oxide nanoparticles using *Eucalyptus lanceolata* leaf litter: Characterization, antimicrobial and agricultural efficacy in maize. *Physiol. Mol. Biol. Plants*., **28**(2): 363-381.

Shibula K and Velavan S (2015). Determination of phytocomponents in methanolic extract of *Annona muricata* leaf using GC-MS technique. *Int. J. Pharm. Phyto. Res.*, **7**(6): 1251-1255.

Sivaranjani T and Meenakshisundaram M (2022). Plant extract-mediated synthesis of ZnO nanoparticles and their applications. *Bioresource Technology Reports*, **9**: 1401-1411.

Stiles LI, Ferrao K and Mehta KJ (2024). Role of zinc in health and disease. *Clem*., **24**(1): 1-19.

Tegenaw AB, Yimer AA and Beyene TT (2023). Boosting the photocatalytic activity of ZnO-NPs through the incorporation of C-dot and preparation of nanocomposite materials. *Heliyon.*, **9**(10).

Umar H, Kavaz D and Rizaner N (2018). Biosynthesis of zinc oxide nanoparticles using Albizia lebbeck stem bark, and evaluation of its antimicrobial, antioxidant, and cytotoxic activities on human breast cancer cell lines. *Int. J. Nanomed*., **14**(4): 87-100.

Vidhya K, Chandirasekaran K, Sivakumar S, Kavitha J and Venkateswari R (2023). Phytochemical screening, GC-MS and antioxidant activity of *Annona muricata*. *Phytochem. Screening*., **18**(2): 18517-18530.

Vignesh M, Kumar S, Natarajan D and Ramesh S (2022). Green synthesis and characterization of zinc oxide nanoparticles using plant extracts: Enhanced antimicrobial and antioxidant activity. *Pak. J. Pharm. Sci.* **35**(3): 587-594.

Xiao F, Xu T, Lu B and Liu R (2020). Guidelines for antioxidant assays for food components. *Food Front.*, **1**(1): 60-69.

Yassin H, Kumar P and Sahu R (2023). Functional groups and structural effects in plant-based ZnO nanoparticle synthesis: Implications for therapeutic applications. *J. Adv. Mater. Res.*, **15**(6): 243-251.

Yassin MT, Al-Askar AA, Maniah K and Al-Otibi FO (2022). Green Synthesis of Zinc Oxide Nanocrystals Utilizing *Origanum majorana* Leaf Extract and Their Synergistic Patterns with Colistin against Multidrug-Resistant Bacterial Strains. *Crystals (Basel).*, **12**(11): 1513.